Design of high-temperature solar-selective coatings based on aluminium titanium oxynitrides $Al_yTi_{1-y}(O_xN_{1-x})$. Part 2: Experimental validation and durability tests at high temperature

Escobar-Galindo, R.; Guillén, E.; Heras, I.; Rincón-Llorente, G.; Alcón-Camas, M.; Lungwitz, F.; Munnik, F.; Schumann, E.; Azkona, I.; Krause, M.;

Design of high-temperature solar-selective coatings based on aluminium titanium oxynitrides $Al_yTi_{1-y}(O_xN_{1-x})$.
Part 2: Experimental validation and durability tests at high temperature

R. Escobar-Galindo[1*], E. Guillén[2], I. Heras[3], G. Rincón-Llorente[4], M. Alcón-Camas[5], F. Lungwitz[6], F. Munnik[6], E. Schumann[6], I. Azkona[7], M. Krause[6]

[1]Departamento de Ciencia de los Materiales e Ingeniería Metalúrgica y Química Inorgánica, IMEYMAT, Universidad de Cádiz, 11510 Puerto Real, Spain

[2]Functional Surfaces and Nanostructures, Profactor GmbH, Im Stadtgut A2, 4407 Steyr-Gleink, Austria

[3]Department of Applied Physics, University of Salamanca, 37008, Salamanca, Spain
[4]IK4-TEKNIKER, Iñaki Goenaga street, 20600 Eibar, Gipuzkoa, Spain
[5]Abengoa Research S. L., Abengoa, Seville, Campus Palmas Altas 41014, Spain
[6]Helmholtz-Zentrum Dresden-Rossendorf, 01314 Dresden, Germany
[7]Metal Estalki S.L., Polígono Ugaldeguren II, 48170 Zamudio, Spain

Abstract

The durability of two solar-selective aluminium titanium oxynitride multilayer coatings was studied under conditions simulating realistic operation of central receiver power plants. The coatings were deposited by cathodic vacuum arc applying an optimized design concept for complete solar-selective coating (SSC) stacks. Compositional, structural and optical characterization of initial and final stacks was performed by scanning electron microscopy, elastic recoil detection, UV-Vis-NIR-IR spectrophotometry and X-Ray diffraction. The design concept of the solar selective coatings was validated by an excellent agreement between simulated and initial experimental stacking order, composition and optical properties.

Both SSC stacks were stable in single stage tests of 12 hours at 650°C. At 800°C, they underwent a structural transformation by full oxidation and they lost their solar selectivity. During cyclic durability tests, multilayer 1, comprised of TiN, $Al_{0.64}Ti_{0.36}N$ and an $Al_{1.37}Ti_{0.54}O$ top layer, fulfilled the performance criterion (PC) $\leq 5\%$ for 300 symmetric, 3 hours long cycles at 600°C in air. Multilayer 2, which was constituted of four $Al_yTi_{1-y}(O_xN_{1-x})$ layers, met the performance criterion for 250 cycles (750 hours), but was more sensitive to these harsh conditions. With regard to the degradation mechanisms, the coarser microstructure of multilayer 1 is more resistant against oxidation than multilayer 2 with its graded oxygen content. These results confirm that the designed SSCs based on $Al_yTi_{1-y}(O_xN_{1-x})$ materials withstand

---

* Corresponding author: Tel +34 956 01 2751; *e-mail address:* ramon.escobar@uca.es (R. Escobar-Galindo)

breakdown at 600ºC in air. Therefore, they can be an exciting candidate material for concentrated solar power applications at high temperature.

1   Introduction

An optimal solar selective coating (SSC) to be used for central receivers in a concentrated solar power (CSP) plant needs to show appropriate optical properties as well as thermal and mechanical stability in air at high temperatures. In particular, coatings applied to central receivers do suffer thermal cycling during plant start-up and stop-down (plant handling) and thermal shocks during cloud transients. Despite the fact that the market of solar absorbers is rapidly increasing [1], a standardisation for the service life prediction is still lacking, in particular for high temperature solar absorber coatings. In the 90's, the International Energy Agency (IEA) in Task X of the Solar Heating and Cooling (SHC) program developed a procedure to simulate the expected service lifetime of the coating over 25 years for low temperature applications (T < 300ºC) [2]. In recent literature [3]-[5], the performance criterion (PC), based on changes in absorptance ($\Delta\alpha$) and emittance ($\Delta\varepsilon_T$) has been updated for high temperature applications (T > 400ºC) and can be described as follows:

$$PC = -\Delta\alpha + 0.5\,\Delta\varepsilon_T \begin{cases} PC \leq 5\ PASS \\ PC > 5\ FAIL \end{cases} \tag{1}$$

This criterion has been found to describe reasonably the ageing of the coatings in many applications [3]-[6] and it was evaluated that a maximum performance decrease of 5% could be acceptable [7]. Based in this procedure a European service life predication standard EN 12975-3-1 (2011) was developed by the European Committee for Standardization [8]. In a very recent review [3], Zhang *et al*. brilliantly summarizes the most applied thermal stability and testing methods (i.e. customized and accelerated ageing standard testing methods). The authors also described thoroughly the main ageing mechanisms, that is, diffusion and oxidation, but also microstructural and compositional changes occurring at high temperatures. They concluded that there is an urgent need of drawing up a broadly applicable test standard for the performance criterion as none of the currently applied testing methods are suitable to predict the service lifetime of solar selective coatings applied in air under high temperature conditions.

Among the potential candidates to be used as solar absorber layers in high temperature applications, Physical Vapour Deposition (PVD) deposited coatings (in particular $Al_yTi_{1-y}(O_xN_{1-x})$ based coatings) have been considered in the literature [9]-[14] due to their proven excellent oxidation resistance and thermal stability e.g. for high temperature machining

applications [15]-[21]. In [14] Du *et al.* reported thermal stability in air up to 400ºC for 192 hours of an Al/Ti$_{0.5}$Al$_{0.5}$N/Ti$_{0.25}$Al$_{0.75}$N/AlN solar selective coating deposited on stainless steel (SS) by magnetron sputtering (MS). Barshilia *et al.* have extensively reported the characterization and high temperature performance of Ti/AlTiN/AlTiON/AlTiO SSCs deposited by MS on SS and copper substrates [10]-[12]. The developed coatings showed a high thermal stability during short periods (2 hours) at 400ºC and after 1000 hours of cyclic heating conditions (using 3ºC/minute as heating and cooling ramps) in air at 350ºC. However, both systems underwent a significant loss of their optical performance at higher temperatures. The main failure mechanisms were identified to be oxidation and diffusion. At 500ºC oxygen and nitrogen diffuse through the columnar structure of the MS deposited AlTiN layers forming Al–Ti-O–N films that destroy the optimized four-layer structure and consequently the optical selectivity of the SSC. In addition, surface colour alterations and delamination problems were observed at T > 600ºC for coatings deposited directly on a Cu substrate [1][12][14]. In order to prevent these failure mechanisms, and to improve oxidation resistance, thermal stability and performance in cutting tests, the incorporation of silicon into the Al-Ti-N layer structure was proposed [22][23]. Following this approach, Rebouta *et al.* [24] showed PC changes below 5% for a SSC multilayer of TiAlSiN/TiAlSiON/SiO$_2$ after 600 hours of thermal treatment at 278ºC in air, while Feng *et al.* [25] reported that TiAlSiN/TiAlSiON/Si$_3$N$_4$ SSCs deposited on SS remained stable after heat treatments at 272ºC in air for 300 h. The combination of multilayers using different nitrides (i.e. TiAlCrN/TiAlN/AlSiN in [26]) resulted in SSCs thermally stable in air up to 400ºC for 4 hours. Barshilia *et al.* recently proposed the use of a more complex stacking structure of TiAlC/TiAlCN/TiAlSiCN/TiAlSiCO/TiAlSiO [27][28], primarily due to the very high thermal stability (up to 1200ºC in air) of the individual constituent layers. Moreover, they reported that the presence of up to 6 interfaces in the system reduces the porosity and helps in blocking the formation of the typical columnar microstructure of sputtered coatings. The designed tandem absorber showed high thermal stability in air up to 500 °C for 2 h and long thermal stability up to 325 °C for 400 h. All these approaches, although valid, apply complicated and expensive processing steps jeopardizing the industrial manufacturing of the proposed SSC structures.

As alternative approach to grow thermally stable SSCs with a simpler design, we recently proposed in [29] the use of Cathodic Vacuum Arc (CVA) to promote the deposition of denser Al$_y$Ti$_{1-y}$(O$_x$N$_{1-x}$) films with less-pronounced or even suppressed columnar morphology in order to improve the performance of the absorber coating when subjected to thermal treatments [30]-[32]. A set of coatings based on compositionally graded Al$_y$Ti$_{1-y}$(O$_x$N$_{1-x}$) layers was designed

and optimized with respect of their final SSC properties [29]. The goal of this second part paper is twofold: i) experimentally validate the SSC designs made in [29] and ii) assess the thermal stability of these multilayer stacks in air. In order to fulfil those objectives complete solar selective multilayers were deposited by CVA. Scanning Electron Microscopy (SEM), Elastic Recoil Detection (ERD), X-Ray diffraction (XRD), UltraViolet-Visible-Near Infrared (UV-Vis-NIR) and Fourier Transform Infrared (FTIR) spectrophotometry were applied for comprehensive compositional, structural and optical characterization. Excellent agreement was found between the nominal properties of the coatings and those of the experimentally deposited stacks, thus validating the designs based on the optical constants of each of the individual oxynitride layers. The thermal stability of these multilayer stacks in air was evaluated by i) single-stage tests of 12 hours at 450, 650 and 800ºC and ii) heating–cooling cycles between 300-600ºC up to 900 hours. Changes observed in the optical performance of the coatings upon thermal treatment were correlated with modifications of layer composition, microstructure, and morphology. The maximum working temperature of the studied multilayer coatings was 250ºC higher than the values reported for this class of materials under comparable conditions until now. Hence, the applied approach for design and development of optical coatings, based on a single-batch process technology, has led to SSCs with competitive properties for realistic operation conditions of central receiver power plants.

2   Experimental details

2.1   Thin film growth

Two SSC multilayer stacks were grown on mirror polished Inconel HAYNES ® 230 and on silicon (100) substrates at 450°C using a commercial direct current (DC) non-filtered CVA PL70 Platit setup. Details of the deposition parameters of the individual $Al_yTi_{1-y}(O_xN_{1-x})$ absorber and antireflective layers were given in the companion paper [29]. A layer of TiN was deposited as an IR reflective film in the SSC stack employing the same experimental setup. The TiN layer was deposited at 300ºC using a 99.99% pure Ti metallic cathode and 3 sccm of N_2 gas flow. The complete SSC stack (TiN IR reflective layer/ $Al_yTi_{1-y}(O_xN_{1-x})$ absorber layer(s)/ AlTiO antireflective layer) was manufactured in a single batch process.

2.2   Thin film characterization

A Hitachi S5200 Scanning Electron Microscope equipped with a field emission gun (FEG) was employed to analyze the morphology of the deposited samples. Cross-sectional and top surface

images of the samples deposited on silicon substrates were measured without metallization at 1 and 5 kV electron beam energy.

ERD analysis was used to determine the depth-resolved elemental composition of the samples. The measurements were carried out using an incident 43 MeV Cl^{7+} ion beam of a 6 MV tandem accelerator. With this experimental setup, the ERD spectra of all elements are obtained, and moreover the RBS spectrum of Ti (and possible heavy element impurities). The spectra were fitted simultaneously using the program NDF v9.3g [33] to obtain profiles of concentration as a function of depth.

The phase structure of the SSCs was determined by X-ray diffraction employing grazing incidence geometry (GIXRD) using a Rigaku Ultima IV diffractometer with Cu-Kα radiation (λ=1.5406 Å). The incident angle was 0.4º, and the XRD patterns were measured in the diffraction angle range of 20–100º in steps of 0.02º.

The reflectance at room temperature was measured under an incident angle of 11º from the normal in the 300 to 2500 nm wavelength range using a Perkin Elmer UV-Vis-NIR spectrophotometer Lambda 1050. A 150-mm integrated sphere accessory consisting of two hemispheres coated with Spectralon and equipped with PMT and InGaAs detectors was employed. Spectralon was used as the diffusively reflecting reference.

Mid IR reflectance was recorded in the wave number (wavelength) range of 400 to 4000 cm^{-1} (2.5 to 25 μm), with a resolution of 0.4 cm^{-1} using a FTIR spectrometer Bruker Vertex 70. The instrument was equipped with a DLaTGS detector and a KBr beam splitter. A specular "W-type" accessory was employed to measure reflectance of mirror like samples, employing a gold coated glass as reference. Additionally, the IR reflectance of rough samples was measured by an integrated sphere accessory coated with gold.

Experimental solar absorptance (α) and thermal emittance ($\mathcal{E}$) of the coatings were evaluated from UV-Vis-NIR and FTIR reflectance spectra as explained in [29].The commercial software CODE [34] was employed to simulate the reflectance spectra using optical constants calculated from experimental data, as explained in [29].

2.3   Durability tests

A specific durability test for the evaluation of thermal stability and ageing properties of high temperature solar selective coatings that simulates realistic operation of central receiver power plants was designed for this work. It comprises i) single-stage and ii) cycling thermal treatment tests.
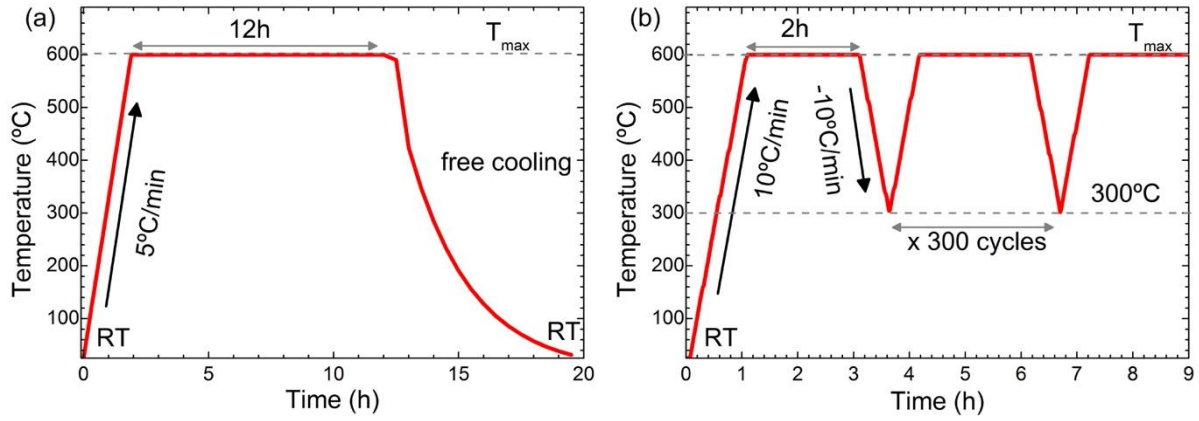
Figure 1.– Schematic illustration of the (a) single-stage and (b) cycling thermal treatment tests applied to the studied SSC stacks. The single stage thermal test is represented for the case T_{max} = 600ºC. Similar tests were performed at 450 and 800ºC.

The single-stage thermal treatment test consists of a single heating cycle in an oven at atmospheric conditions where the selected temperature (450, 650 or 800ºC) is kept constant for 12 hours. These temperatures were selected as the current working temperature in parabolic trough plants is 450ºC while in tower plants the current target temperature is 650ºC for molten salts and 800ºC for heat transfer fluids (currently) under development, respectively. A constant heating ramp of 5ºC/min is applied to reach the desired temperature. After 12 hours, the sample is cooled down to room temperature inside the oven (Figure 1(a)). This treatment is related to the accelerated degradation test commonly used in the literature [1] to assess the thermal stability of the coatings and will be used to set the maximum temperature at which the more representative cycling thermal tests should be performed. The furnace employed for this test was a Nabertherm L9/11 with controller P330, equipped with SiC rod.

The scheme of the cycling thermal tests is shown in Figure 1(b). The samples were heated up with a ramp of 10ºC/min to 600ºC in a programmable furnace at atmospheric conditions. Then, they were kept at 600ºC for 2 hours and subsequently cooled down to 300ºC, with a cooling ramp of 10ºC/min. This cycle was repeated 300 times for a total experimental time of 900 hours, which gives 600 hours at maximum temperature and 300 hours within the heating and cooling ramps. The samples were visually inspected and optically characterized every 50 cycles. The applied cycling procedure is significantly more severe (i.e. heating and cooling ramps are three times faster) than other reported in literature [12]. Hence, in our opinion, it represents a more realistic test for SSCs since the experimental conditions (i.e. heating and cooling ramps, minimum and maximum temperatures) were selected to be representative for operation conditions in a CSP plant. The programmable furnace employed for the cycling tests was a

Hobersal 13PR/300F with adjustable cooling and heating ramp provided by an Eurotherm controller.

3 Results and discussion

3.1 Characterization of as-deposited complete SSCs

The individual $Al_yTi_{1-y}(O_xN_{1-x})$ layers used for the design of the complete SSC stacks were extensively described and characterized in part 1 of the publication [29]. Here a simplified notation is applied for the description of the deposited solar selective multilayers (Table 1). AlTiN #1 represents a layer of the composition $Al_{0.64}Ti_{0.36}N$, AlTiO #6 stands for the $Al_{1.37}Ti_{0.54}O$ antireflective top layer and AlTiON #4 has the nominal composition $Al_{0.65}Ti_{0.35}(O_{0.26}N_{0.74})$ [29].

Table 1.- Description of the deposited multilayer SSC structure. The error in the experimental thickness measurements obtained by SEM is ± 5 nm.

Sample #	Coating structure	Nominal Thickness (nm)	Experimental Thickness (nm)
Multilayer 1	AlTiO #6	66	60
	AlTiN #1	120	120
	TiN	400	330
Multilayer 2	AlTiO #6	64	60
	AlTiON #4	55	150
	AlTiN #1	105	
	TiN	400	345

The cross-sectional morphology of the two as-deposited multilayers was analysed by SEM after cleavage of the samples using liquid nitrogen. No delamination is observed neither between the substrate and the TiN IR layer, nor between the layers that comprises the $Al_yTi_{1-y}(O_xN_{1-x})$ stack (Figure 2). The thicknesses of the different individual layers are included in the SEM images. The deposited thicknesses of multilayer 1 (ML1 in Figure 2 (a)) were in good agreement with the nominal individual values (see Table 1). For multilayer 2 (ML2 in Figure 2 (b)), only three different layers can be distinguished by SEM. As the total thickness of the deposited SSC and the sum of AlTiON #4 and AlTiN #1 is very close to the nominal one, we are prone to confirm that the four individual layers of multilayer 2 were properly deposited. Moreover, ERD data and the full agreement between measured and simulated reflectance spectra confirm the deposition of AlTiON#4 (see below).
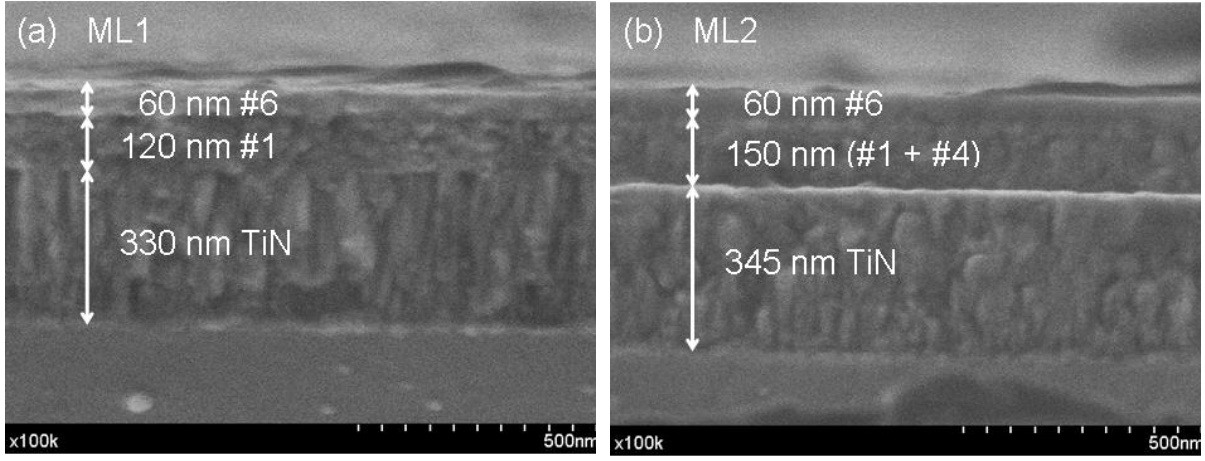
Figure 2.- SEM cross-sectional images of deposited SSCs: (a) multilayer 1 (ML 1) and (b) multilayer 2 (ML 2). The measured thickness and layer distribution are indicated in the images.

In Figure 3, the ERD profiles of the as-deposited multilayers are shown. The three layers of multilayer 1 are clearly identified in Figure 3 (a). It is worth noting that there is no sharp interface between the AlTiO #6 and the AlTiN #1 layers. This is in part because of the limited detector resolution and energy straggling of the ions (statistical variation of the energy loss of ions in matter). The difference between these contributions and the slopes of the profiles can be attributed to a non-zero interface width and this will be discussed in detail when describing the optical characterization. In the case of multilayer 2, also the oxynitride layer #4 can be identified. In both cases there is evidence for oxygen contamination at the AlTiN/TiN interface with a corresponding drop in the nitrogen concentration.
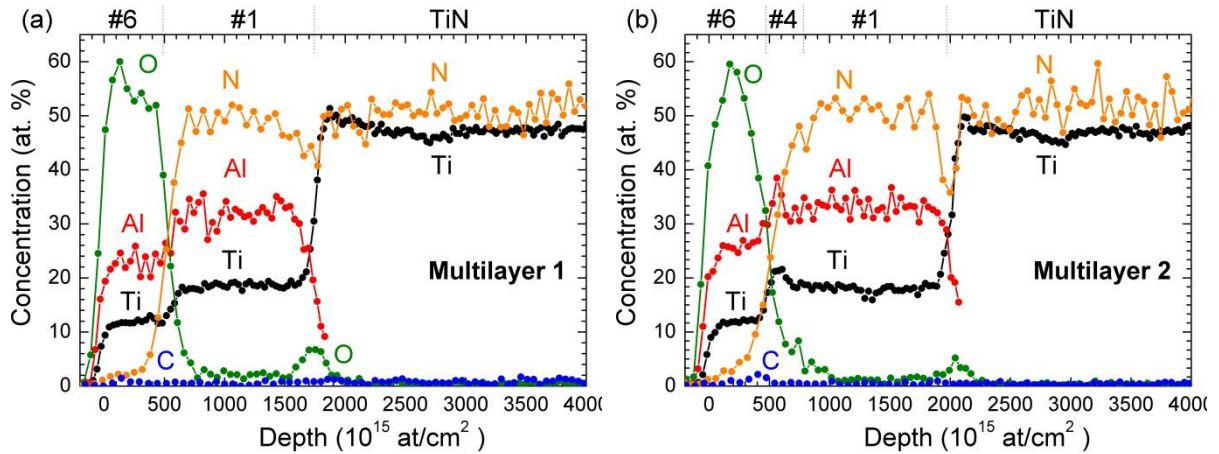

Figure 3.- ERD profiles of the as-deposited SSCs: (a) multilayer 1 and (b) multilayer 2. The layer structure of the multilayers is represented on the top of each graph.

The reflectance of the multilayer stacks was measured by UV-Vis–NIR and FTIR spectrophotometry in the range of 0.3 – 25 μm. In Figure 4, the experimental and simulated reflectance spectra of the two designed multilayer stacks are compared. Both samples present

the typical dark blue colour of SSCs (see photo insets in Figure 4). The simulation results are based on the optical models developed in part 1 of this work [29]. The absorptance and emittance data obtained both from simulation and the experiments are displayed in Table 2.
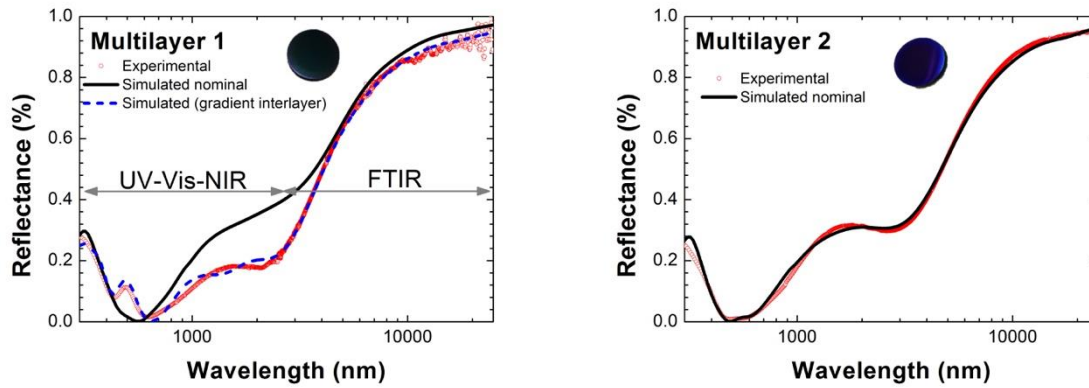

Figure 4.- Simulated and experimental reflectance spectra of SSCs: (a) multilayer 1 and (b) multilayer 2. Photographs of the as deposited SSC samples are included.

Table 2.- Simulated and measured solar absorptance (α) and thermal emittance (ε_{RT}) of SSCs based on $Al_yTi_{1-y}(O_xN_{1-x})$.

	Multilayer 1		Multilayer 2	
	α (%)	ε (%)	α (%)	ε (%)
Simulated	87.7	10.0	88.6	13.6
Simulated (gradient interlayer)	90.1	12.8	--	--
Experimental	91 ± 1	14 ± 1	89 ± 1	13 ± 1

There are clear differences between the simulated and experimental reflectance spectra of multilayer 1 (see Figure 4(a)). These changes lead to deviations of +3.3 % and +4 % between experimental and simulated absorptance and emittance, respectively, which are larger than the experimental error (± 1%). It is worth noting that optical simulations performed by CODE assume the presence of sharp interfaces between the different layers in the deposited stack. However, this is not the case for multilayer 1 as revealed by the ERD profile of Figure 3 (a). In this case, a gradual change of reactive gas flows from a pure nitride (AlTiN) to a pure oxide film (AlTiO) causes a gradient-like instead of a sharp transition of the layer composition. This relatively smooth compositional change accounts for the observed deviation of the experimental optical constants. This hypothesis is proven by a new simulation of multilayer 1 that was performed by introducing a gradient interlayer of 138 nm using the optical constants of the oxynitride layers (48 nm #5/ 72 nm #4/ 18 nm #1) derived in [29]. As a result, the agreement

of experimental and simulated reflectance spectrum of multilayer 1 with the incorporation of the interlayer was significantly improved (see dotted line in Figure 4(a)). The improvement of the simulation is directly reflected in the absorptance and emittance values, which agree with the simulated ones within the experimental error (see Table 2).

In the case of multilayer 2 the presence of the intermediate oxynitride layer #4 acts as a transition zone between the pure nitride AlTiN #1 and oxide AlTiO #6 layers, and thus, the simulated spectrum properly fits to the experimental one (see Figure 4b). Accordingly, the experimental absorptance and emittance values match the target values within the measurement uncertainty (see Table 2). These results show once again the strength and validity of the optical simulations performed in this work.

3.2 Single-stage thermal treatment tests of complete solar selective coatings

Following the successful validation of the SSCs, their thermal stability and ageing properties were investigated by exposing the samples to single-stage and cycling thermal treatment tests described in section 2.3. The compositional, microstructural and optical properties of the samples were characterized after each thermal treatment step.

Figure 5 (a) and (b) show the reflectance spectra of the deposited multilayers after deposition and 12 hours single-stage thermal treatment tests at 450, 650 and 800ºC.
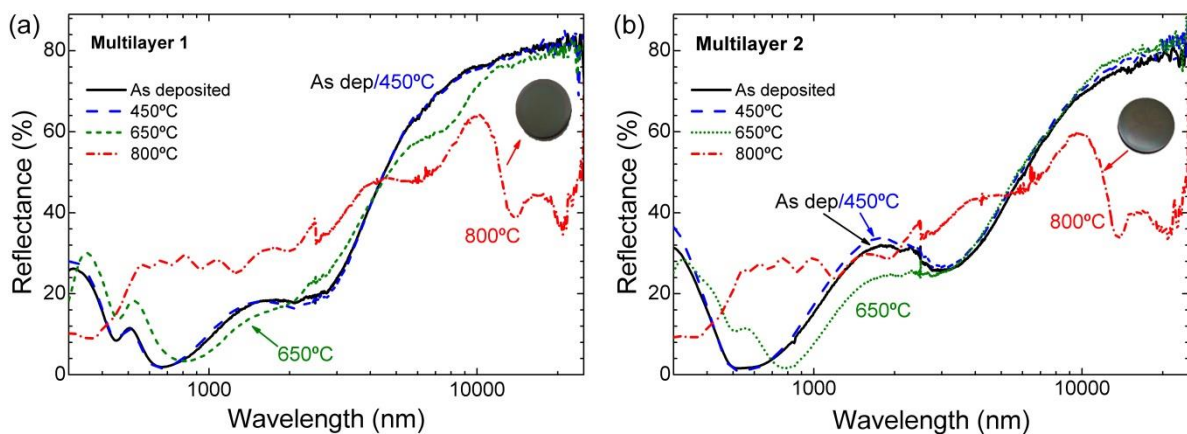

Figure 5.- Reflectance of (a) multilayer 1 and (b) multilayer SSCs as deposited and after single-stage thermal treatments. The photographs of the degraded SSCs after the thermal test at 800ºC are included.

In Figure 6(a) and (b) the variations in the solar absorptance and thermal emittance for both multilayers are plotted. No significant changes were observed for the multilayers after 12 hours at 450ºC. The annealing at 650ºC resulted in a detrimental optical performance decrease for multilayer 1 ($\Delta\alpha$ = -2.2%, $\Delta\varepsilon$ = +2.7), while that of multilayer 2 improved ($\Delta\alpha$ = +0.3 %, $\Delta\varepsilon$ =

-3.1). Both multilayers fulfil the defined performance criteria of thermal stability (PC ≤ 5, equation (1)) after the thermal treatments up to 650ºC (Figure 6(c) and Table S.1 (see Supplementary information).
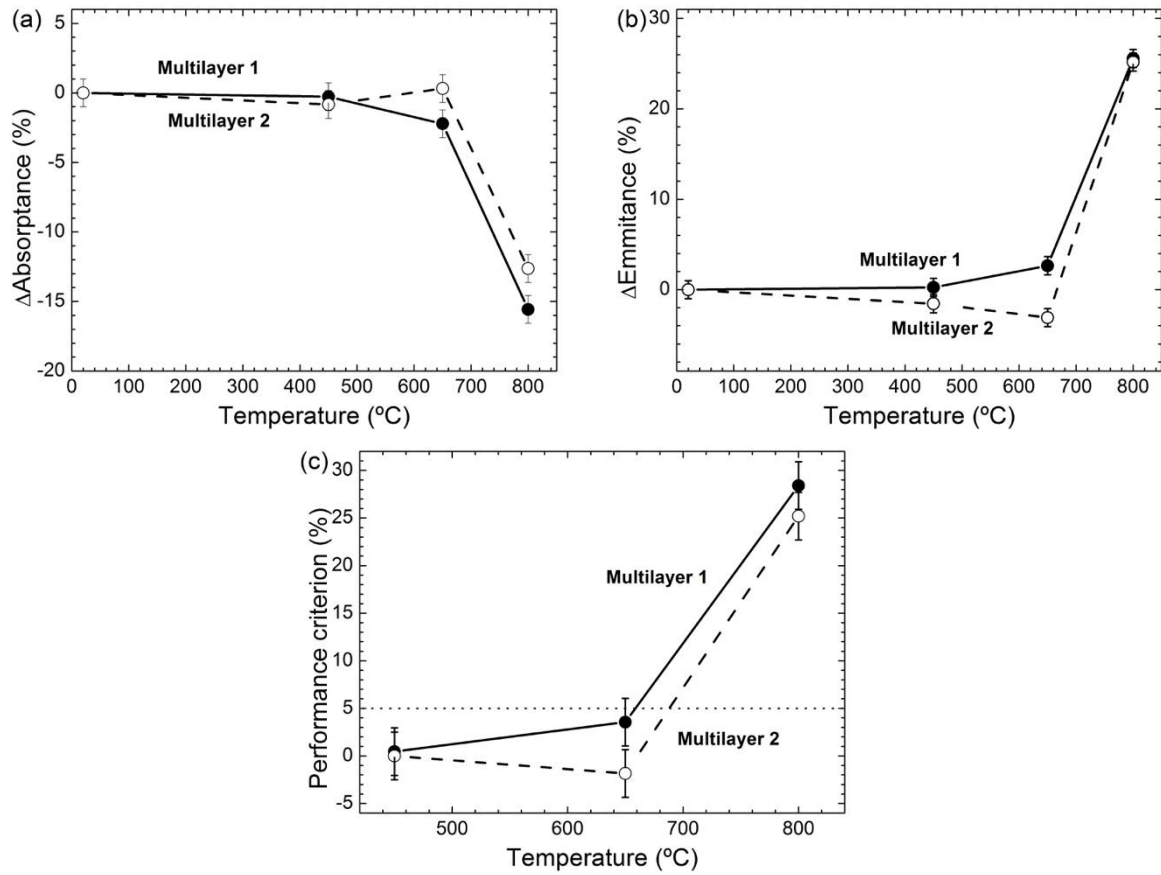

Figure 6.- Variation of the (a) α, (b) ε and (c) performance criterion measured after the single-stage thermal tests performed at 450, 600 and 800ºC for multilayer 1 (solid line) and multilayer 2 (dashed line). In (c) a horizontal dotted line is plotted to mark the threshold of PC = 5%.

A drastic change in the reflectance spectra was observed after the thermal treatment at 800ºC (see Figure 5). The performance criterion (PC > 25) clearly exceeds the defined limit for passed, and hence, both SSCs fail under these conditions (equation (1)) (see Table S.1 and Figure 6). The reflectance change is accompanied by a change of the sample's colour from dark blue to yellowish-brown (see photo inset in Figure 5). Du *et al.* observed a similar degradation for Al/$Ti_{0.5}Al_{0.5}$N/$Ti_{0.25}Al_{0.75}$N/AlN solar selective coating [1] [14] but under less severe conditions (2 hours at 500ºC). In order to correlate the changes of the optical properties with microstructural changes, the heat-treated multilayers were analysed by GIXRD and ERD.
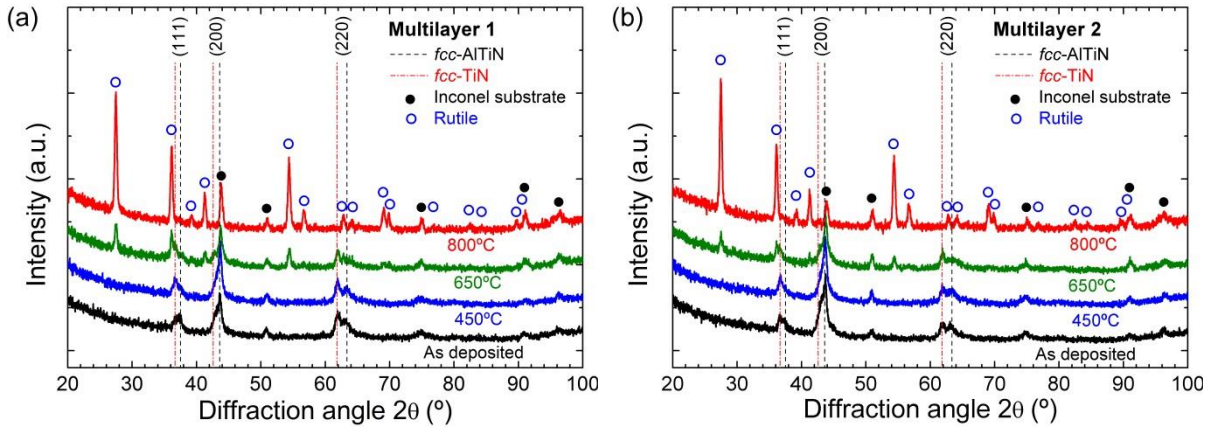
Figure 7.- GIXRD patterns of the SSCs as deposited and after thermal treatment for 12 hours at 450ºC, 650ºC and 800ºC of (a) multilayer 1 and (b) multilayer 2. The vertical lines indicate the peak positions for fcc-$Al_{0.5}Ti_{0.5}N$ and TiN (ICCD card numbers 04-018-6856 and 00-038-1420, respectively). The position of rutile and Inconel diffraction peaks are also shown with open and solid circles, respectively.

After single-stage thermal treatment at 450°C the GIXRD patterns of ML1 and ML2 did not show significant changes compared to those of the as-deposited multilayers. All observed peaks were assigned to fcc-AlTiN, that was found to give identical patterns to AlTiON #4 and TiN (ICCD card numbers 04-018-6856 and 00-038-1420, respectively) and to the Inconel substrate. The doublet-like structure of the TiN and AlTiN #1/ AlTiON #4 peaks is caused by small lattice parameter differences of their NaCl-type crystal structure. No peaks of AlTiO are found in agreement with the observations in [29]. Diffraction peaks of rutile TiO_2 (ICCD card 021-1276) appeared after the temperature was increased to 650ºC (see Figure 7). After this treatment step the initial crystallographic TiN and AlTiON phases were still present in the samples as it is most clearly seen from the (220) peaks of TiN and AlTiN at 61.81º and 63.37º, respectively. After the treatment at 800°C the diffractogram showed no more peaks related to nitride phases. Only TiO_2 rutile and Inconel peaks were observed, being more intense for multilayer 1. No other crystalline oxide phases were detected after this treatment step.
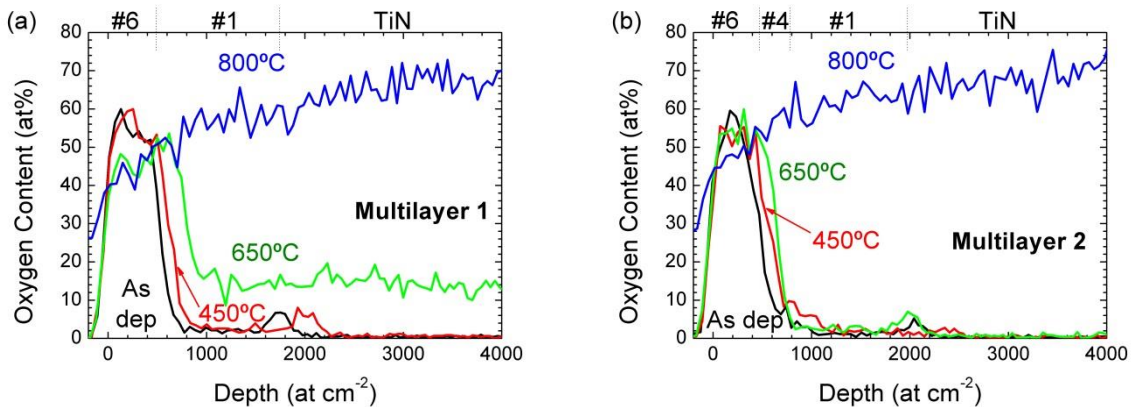
Figure 8.- ERD oxygen profiles of (a) multilayer 1 and (b) multilayer 2 SSCs after single-stage thermal tests.

ERD measurements performed after the 12 hours single-stage tests at 450ºC showed no significant changes in the oxygen profiles of both multilayers (see Figure 8). After exposure to 650ºC, i) a noteworthy broadening of the oxygen profile peak towards the AlTiN #1 and TiN layers and ii) a constant oxygen concentration of about 15 at.% throughout the entire AlTiN #1 and TiN layer stack was observed for multilayer 1. This represents a clear indication of the initial oxidation process of the sample, and is in agreement with the coexistence of rutile and nitride phases as observed in XRD (Figure 7(a)). Furthermore, these structural changes are responsible for the first stages of optical performance degradation of the multilayer (see Table S.1 and Figure 6). On the other hand, the thermal annealing at 650ºC only caused a slight increase in the width of the oxygen profile of multilayer 2. This is in good accordance with the smaller intensity of the rutile peaks in XRD (see Figure 7b) and the better optical performance of multilayer 2 (see Table S.1 and Figure 6) with respect to multilayer 1 after 650°C treatment. After the treatment at 800ºC a complete oxidation of both SSC multilayers has occurred that correlates with the composition ($\sim$ 65% at. oxygen), the intense XRD peaks of rutile (Figure 7) and the worse optical performance of both samples.

Hence, these single-stage tests set a maximum working temperature of 650ºC for both designed SSCs. This temperature is 50ºC and 250ºC higher than the best short-term (2 hours) and long-term (192 hours) thermal experiments reported earlier for AlTiN/AlTiON/AlTiO SSC deposited by MS in [12] and [14], respectively. In the next section, the results of the cycling thermal tests are presented. Thereby, the multilayer SSCs were subjected to 300 thermal cycles (corresponding to a total of 900 testing hours) in air from 300 to 600ºC according to the scheme of Figure 1(b).

3.3   Cycling thermal treatment tests of complete solar selective coatings

The reflectance spectra of the SSC multilayers were measured after every 50 cycles (Figure 9) corresponding to 150 hours of continuous testing. Figure 10 and Table S.2 (supplementary information) summarize the evolution of α and ε with increasing number of thermal treatment cycles.
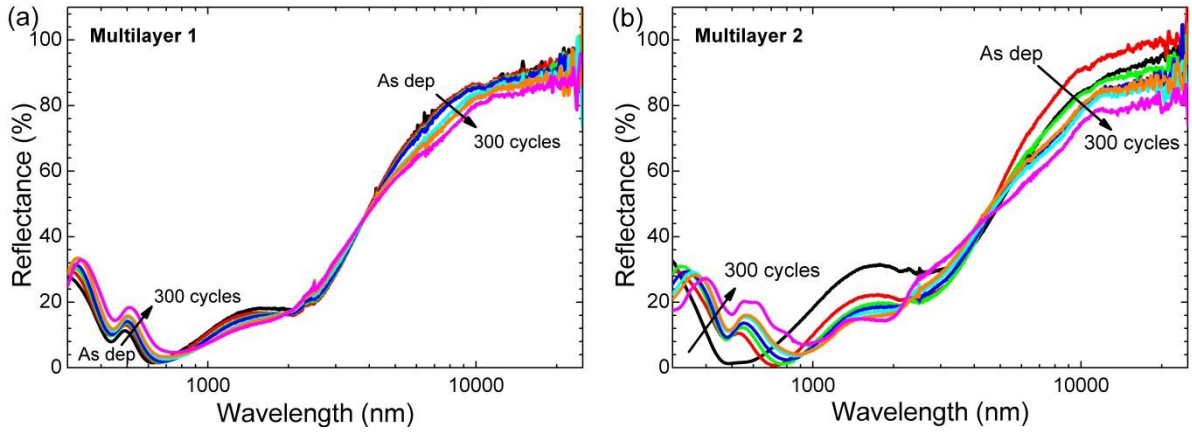
Figure 9.- Reflectance spectra of the (a) multilayer 1 and (b) multilayer 2 as a function of thermal treatment cycles at 600ºC. Each cycle comprised 2 hours at 600°C and symmetric heating and cooling ramps of 10ºC/min between 300°C and 600°C.

The change of the optical performance with the temperature is different for multilayer 1 and multilayer 2. A subtle but continuous diminution of the absorptance and increase of the emittance with increasing number of annealing cycles is found for multilayer 1. On the contrary, for multilayer 2, a clear change in the reflectance spectrum is already observed after the first 50 cycles (150 hours). This change results in an initial improvement of the optical properties (see Figure 10) but it gives an indication that multilayer 2 is thermally less stable than multilayer 1, probably due to the more complex layer re-accommodation upon cycling. In the accelerated ageing standard testing method [1], a maximum of 600 hours of testing time is proposed for a coating to fulfil the performance criterion. In our case, minor variations were observed in the optical properties of both multilayer 1 ($\Delta\alpha$ = -1.0 %, $\Delta\varepsilon$ = +3.9 %), and multilayer 2 ($\Delta\alpha$ = -0.4 %, $\Delta\varepsilon$ = +5.4 %) even after 250 thermal cycles (750 hours). This results in excellent optical performance with PC values below the threshold (PC ~ 3) for both coatings. However, in Figure 10 (c) it can also be seen that the PC value of multilayer 2 decreases faster (~3 times) than that of multilayer 1, confirming the differences in the thermal stability of both samples. Multilayer 1 still passes satisfactorily the test (PC = 5.0) after 900 hours of thermal cycling. For multilayer 2 a sudden decrease of absorptance (-2.5%) and increase of emittance (+11.6 %) leads to a performance criterion (PC = 9.5) clearly above the defined threshold (see Figure 10(c)).
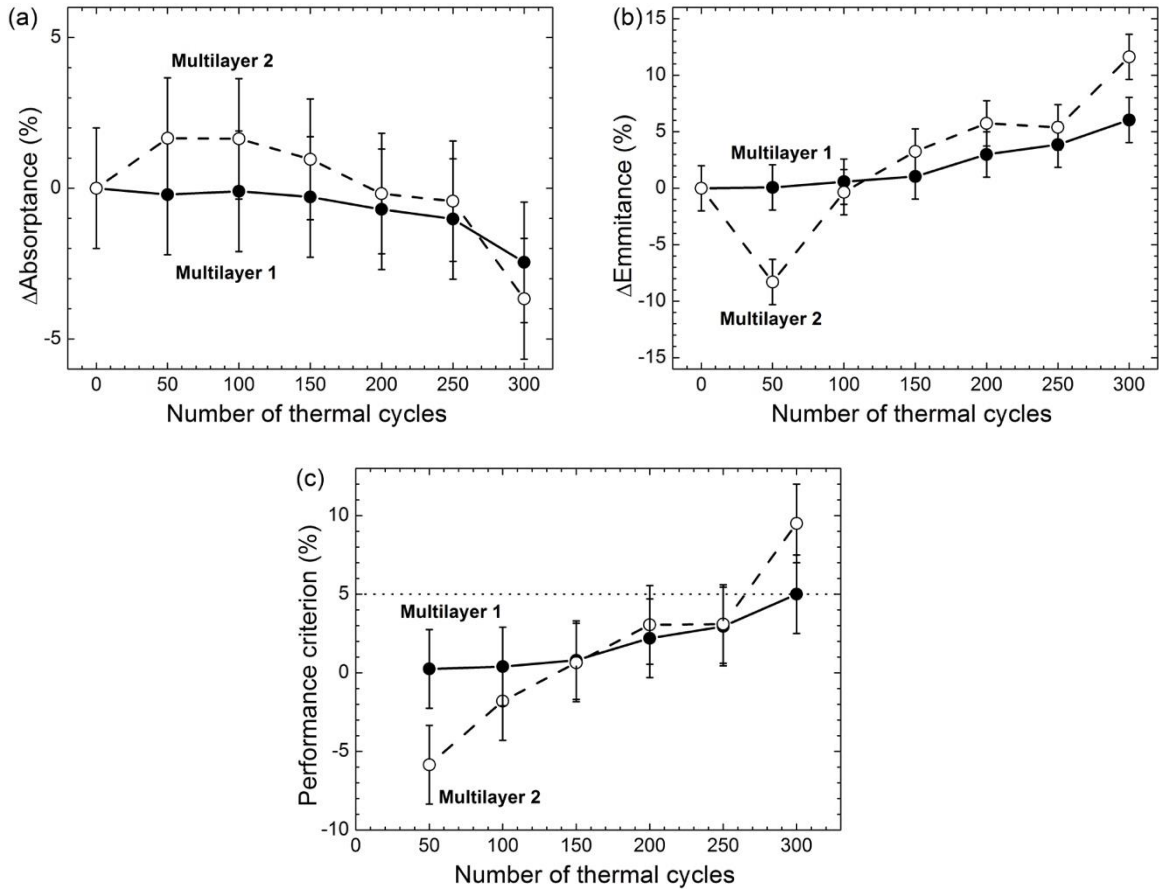
Figure 10.- Variation of (a) α, (b) ε and (c) performance criterion of ML1 (solid line) and ML2 (dashed line) as a function of thermal treatment cycles at 600ºC. The dotted line at PC = 5% marks the borderline between passed and failed test according to equation (1).

The changes of the optical properties of ML 1 and ML 2 go along with microstructural changes that are visible in the GIXRD diffractograms measured before and after 300 thermal cycles (Figure 11). Similar to the single-stage tests, rutile peaks are observed after 900 hours of thermal cycling tests (300 cycles). These peaks are more evident for multilayer 2, reinforcing the hypothesis that the degradation of this SSC is due to the permeation of oxygen through the multilayer structure.
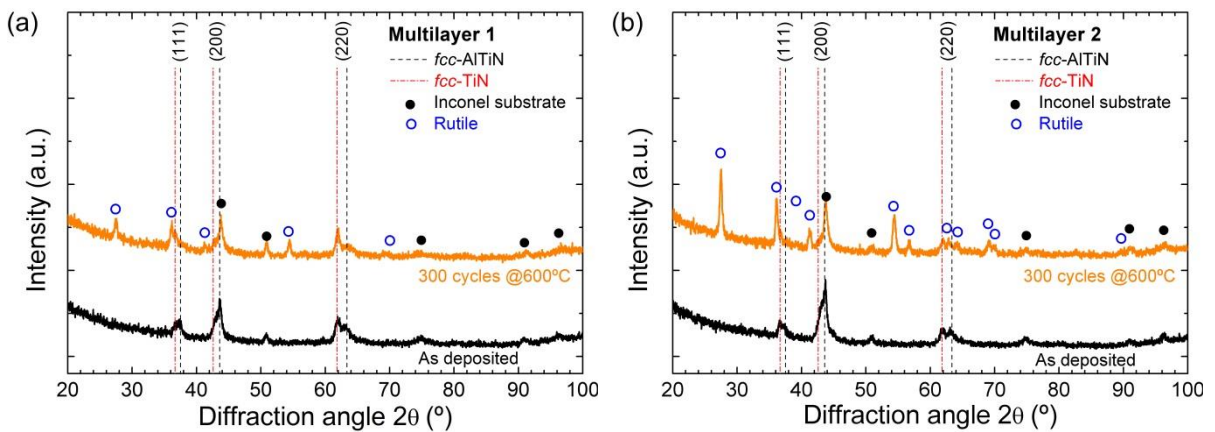
Figure 11.- GIXRD patterns of the SSCs as deposited and after 300 symmetrical thermal cycles (900 hours between 300-600ºC) of (a) multilayer 1 and (b) multilayer 2. The position of rutile and Inconel diffraction peaks are also shown with open and solid circles, respectively.

Cross sectional SEM images in Figure 12 (a) and (b) show a 10% increase of the thickness of the multilayers probably related to volume expansion due to the oxide formation. In addition, EDX elemental mapping confirms the presence of TiO_2 particles of the top surface of multilayer 1 after cycling (see S.3 in supplementary information). It should be noted that an excellent adhesion was found for both multilayers after the 900 hours of thermal cycling as no delamination was detected neither between the absorber layers stack nor between the TiN layer and the Inconel substrate.
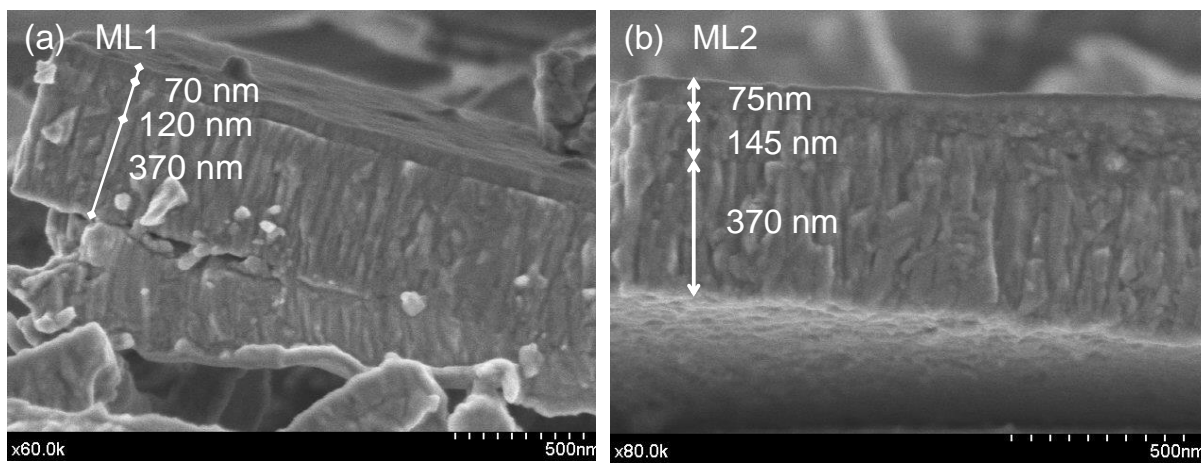

Figure 12.- SEM cross-section images of (a) multilayer 1 and (b) multilayer 2 after symmetrical thermal cycling tests.

Finally, the ERD oxygen profiles of both samples after 300 symmetrical cycles (see Figure 13) confirm the initial oxidation of the AlTiN #1 and TiN layers. In particular, in multilayer 2 there is a clear increase in the oxide scale thickness probably due to the presence of the intermediate oxynitride layer. A detailed analysis of the $Al_yTi_{1-y}(O_xN_{1-x})$ layer microstructure was performed in [29]. An identical rocksalt-type lattice microstructure was found for layers #1, #4 and 5, with a continuous reduction in the crystallite size with the incorporation of oxygen in the layers. Thus, with regard to the degradation mechanism, the coarser microstructure of multilayer 1 was found to be more resistant against oxidation under long-term cycles than multilayer 2 with its graded oxygen content.
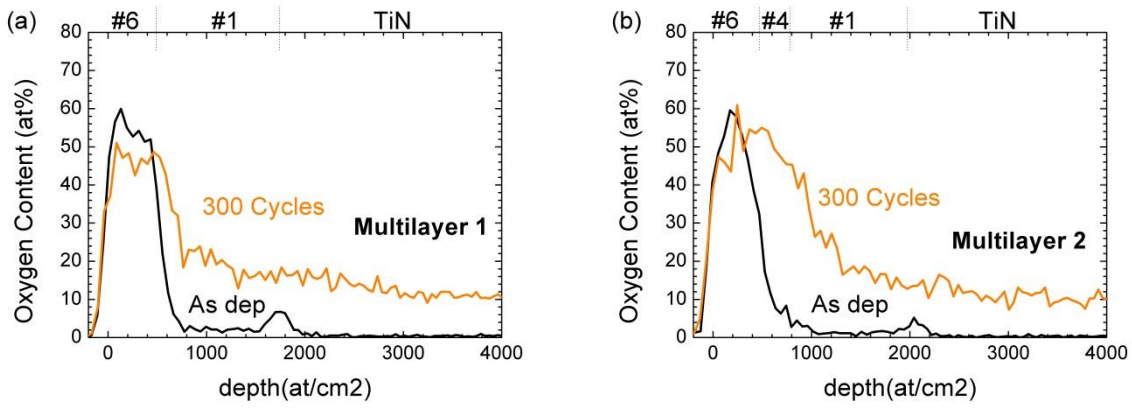
Figure 13.- ERD oxygen profiles of (a) multilayer 1 and (b) multilayer 2 SSCs after 300 cycles.

Hence, very encouraging thermal stability results were obtained for the $Al_yTi_{1-y}(O_xN_{1-x})$ based SSC stacks deposited by CVA, as no significant degradation was found after cycling 900 hours at 600ºC in air for the simpler AlTiO/AlTiN/TiN design. This is by 250 degrees higher than thermal stability values reported for AlTiON based SSC stacks deposited by magnetron sputtering under less severe cyclic heating conditions (3ºC/min heating-cooling ramps) [12]. However, further tests, including thermal shocks, should be performed on the samples to validate its use in a real CSP plant.

4   Conclusions

Two solar-selective aluminium titanium oxynitride multilayer coatings were deposited by cathodic vacuum arc in a single batch process to validate the optimized design concept developed in part 1 of this work [29]. An excellent agreement between simulated and experimental stacking order, composition and optical properties was found. Deviation between experimental and simulated reflectance spectra were resolved by assuming a deposition technique-induced composition gradient of the $Al_yTi_{1-y}(O_xN_{1-x})$ coating without well-defined interfaces.

Both multilayer stacks showed good thermal stability (PC < 4) up to 12 hours of single stage treatment at 650ºC in air. Noticeable oxidation to crystalline rutile TiO_2 was identified by GIXRD and ERD profiles after treatment at 800ºC, which leads to degradation of the optical properties. Samples were subsequently subjected to symmetric thermal cycles in air between 300 and 600ºC with heating and cooling ramps of 10ºC/min. Multilayer 1, comprised of TiN, $Al_{0.64}Ti_{0.36}N$ and an $Al_{1.37}Ti_{0.54}O$ top layer, fulfilled the performance criterion of PC ≤ 5% for 300 cycles (900 hours). On the other hand, multilayer 2, which was constituted of four $Al_yTi_{1-y}(O_xN_{1-x})$ layers, met the performance criterion for 250 cycles (750 hours), but was more sensitive to these harsh conditions at longer times.

These results confirm that the designed SSCs based on dense and coarse $Al_yTi_{1-y}(O_xN_{1-x})$ materials deposited by CVA withstand breakdown at 600ºC in air during cycle tests and are exciting candidate material for CSP applications at high temperature. Moreover, the obtained results highlight the urgent need of a suitable standardization for the thermal stability evaluation of SSCs at high temperatures. In this regard, we proposed a thermal cycling test with experimental conditions (i.e. heating and cooling ramps, minimum and maximum temperatures) selected to be representative of operation conditions in a CSP plant.

5   Acknowledgments

References

[1]   Technology Roadmap: Solar Thermal Electricity-2014 ed. ⟨http://www.iea.org/publications/freepublications/publication/technology-roadmap-solar-thermal-electricity—2014-edition.html⟩. [Last accessed on 02.04.16].

[2]   B. Carlsson, U. Frei, M. Köhl, K. Moller, Accelerated Life Testing of Solar Energy Materials, Case study of some selective solar absorber coating materials for DHW Systems, IEA technical report of Task X in the Soar Heating and Cooling Programme. SP-Report 94:13, 1994. Available from Swedish National Testing and Research Institute, P.O. Box 857, S-50115 Boras, Sweden.

[3]   K. Zhang, L. Hao, M. Du, J. Mi, J-N. Wang, J-P. Meng. A review on thermal stability and high temperature induced ageing mechanisms of solar absorber coatings. Renewable and Sustainable Energy Reviews 67 (2017) 1282-1299

[4]   P. Song, Y. Wu , L. Wang, Y. Sun, Y. Ning, Y. Zhang, B. Daia, E. Tomasella, A. Bousquet, C. Wang. The investigation of thermal stability of Al/NbMoN/NbMoON/SiO2 solar selective absorbing coating. Solar Energy Materials and Solar Cells 171 (2017) 253–257

[5]   O. Raccurt, F. Matino, A. Disdier, J. Braillon, A. Stollo, D. Bourdon, A. Maccari. In air durability study of solar selective coating for parabolic trough technology. AIP Conference Proceedings 1850 (2017) 130010

[6]   M. Köhl, M. Heck, S. Brunold, U. Frei, B. Carlsson, K. Möller. Advanced procedure for the assessment of the lifetime of solar absorber coatings. Sol. Energy Mater. Sol. Cells 2004; 84: 275–89.

[7]   M. Koehl. Durability of solar energy materials. Renew. Energy 2001; 24: 597–607.

[8]   Standardization ECf. Draft BSEN 12975-3-1 thermal solar systems and components –Solar collectors – Part 3-1. Qualification of solar absorber surface durability; 2011. p. 1-34.

[9]   A. Schuler, P. Reimann, P. Oelhafen, G. Francz, T. Zehnder, M. Duggelin, et al., Structural and optical properties of titanium aluminum nitride films ($Ti_{1-x}Al_xN$), J. Vac. Sci. Technol. A. 19 (2001) 922.

[10]   H.C. Barshilia, N. Selvakumar, K.S. Rajam, D. V. Sridhara Rao, K. Muraleedharan, A. Biswas, TiAlN/TiAlON/Si_3N_4 tandem absorber for high temperature solar selective applications, Appl. Phys. Lett. 89 (2006) 191909

[11]   H.C. Barshilia, N. Selvakumar, K.S. Rajam, A. Biswas, Optical properties and thermal stability of TiAlN/AlON tandem absorber prepared by reactive DC/RF magnetron sputtering, Sol. Energy Mater. Sol. Cells. 92 (2008) 1425–1433.

[12]   H.C. Barshilia, Growth, characterization and performance evaluation of Ti/AlTiN/AlTiON/AlTiO high temperature spectrally selective coatings for solar thermal power applications, Sol. Energy Mater. Sol. Cells. 130 (2014) 322–330.

[13]   L. Rebouta, A. Pitães, M. Andritschky, P. Capela, M.F. Cerqueira, A. Matilainen, et al., Optical characterization of TiAlN/TiAlON/SiO_2 absorber for solar selective applications, Surf. Coatings Technol. 211 (2012) 41–44.

[14]   M. Du, X. Liu, L. Hao, X. Wang, J. Mi, L. Jiang, et al., Microstructure and thermal stability of $Al/Ti_{0.5}Al_{0.5}N/Ti_{0.25}Al_{0.75}N/AlN$ solar selective coating, Sol. Energy Mater. Sol. Cells. 111 (2013) 49–56.

[15] T. Leyendecker, O. Lemmer, S. Esser, J. Ebberink, The development of the PVD coating TiAlN as a commercial coating for cutting tools, Surf. Coatings Technol. 48 (1991) 175–178.

[16] F. Vaz, L. Rebouta, M. Andritschky, M.F. da Silva, J.C. Soares, Thermal oxidation of $Ti_{1-x}Al_xN$ coatings in air, J. Eur. Ceram. Soc. 17 (1997) 1971–1977.

[17] J.L. Endrino, G.S. Fox-Rabinovich, R. Escobar Galindo, W. Kalss, S. Veldhuis, L. Soriano, J. Andersson, A. Gutiérrez, Oxidation post-treatment of hard AlTiN coating for machining of hardened steels, Surf. Coat. Technol. 204 (2009) 256-262.

[18] Y. Birol, D. İsler, Thermal cycling of AlTiN- and AlTiON- coated hot work tool steels at elevated temperatures, Mater. Sci. Eng. A528 (2011) 4703-4709.

[19] L. Chen, J. Paulitsch, Y. Du, P.H. Mayrhofer, Thermal stability and oxidation resistance of Ti-Al-N coatings, Surf. Coat. Technol. 206 (2012) 2954–2960

[20] C. Århammar, J.L. Endrino, M. Ramzan, D. Horwat, A. Blomqvist, J.-E. Rubensson, et al., Probing temperature-induced ordering in supersaturated $Ti_{1-x}Al_xN$ coatings by electronic structure, Surf. Coatings Technol. 242 (2014) 207–213.

[21] J. Nohava, P. Dessarzin, P. Karvankova, M. Morstein, Characterization of tribological behavior and wear mechanisms of novel oxynitride PVD coatings designed for applications at high temperatures, Tribol. Int. 81 (2015) 231–239.

[22] S. Carvalho, L. Rebouta, E. Ribeiro, F. Vaz, C.J. Tavares, E. Alves, N.P. Barradas, J.P. Riviere, Structural evolution of Ti-Al-Si-N nanocomposite coatings, Vacuum 83 (2009) 1206–1212

[23] S.Q. Wang, L. Chen, B. Yang, K.K. Chang, Y. Du, J. Li, et al., Effect of Si addition on microstructure and mechanical properties of Ti–Al–N coating, Int. J. Refract. Met. Hard Mater. 28 (2010) 593–596.

[24] L. Rebouta, P. Capela, M. Andritschky, A. Matilainen, P. Santilli, K. Pischow, et al., Characterization of TiAlSiN/TiAlSiON/SiO2 optical stack designed by modelling calculations for solar selective applications, Sol. Energy Mater. Sol. Cells. 105 (2012) 202–207.

[25] J. Feng, S. Zhang, Y. Lu, H. Yu, L. Kang, X. Wang, et al., The spectral selective absorbing characteristics and thermal stability of SS/TiAlN/TiAlSiN/Si_3N_4 tandem absorber prepared by magnetron sputtering, Sol. Energy. 111 (2015) 350–356

[26] K. Valleti, D. Murali Krishna, S.V. Joshi, Functional multi-layer nitride coatings for high temperature solar selective applications, Sol. Energy Mater. Sol. Cells. 121 (2014) 14–21.

[27] J. Jyothi, H. Chaliyawala, G. Srinivas, H.S. Nagaraja, H.C. Barshilia, Design and fabrication of spectrally selective TiAlC/TiAlCN/TiAlSiCN/TiAlSiCO/TiAlSiO tandem absorber for high-temperature solar thermal power applications, Sol. Energy Mater. Sol. Cells. 140 (2015) 209–216.

[28] J. Jyothia, Audrey Soum-Glaude, H.S. Nagaraja, H. C. Barshilia, Measurement of high temperature emissivity and photothermal conversion efficiency of TiAlC/TiAlCN/TiAlSiCN/TiAlSiCO/TiAlSiO spectrally selective coating, Sol. Energy Mater. Sol. Cells 171 (2017) 123–130.

[29] I. Heras, E. Guillén, F. Lungwitz, G. Rincón-Llorente, F. Munnik, E. Schumann, I. Azkona, M. Krause, R. Escobar-Galindo, Design of high-temperature solar-selective coatings based on aluminium titanium oxynitrides $Al_yTi_{1-y}(O_xN_{1-x})$. Part 1: Advanced microstructural characterisation and optical simulation. Solar Energy Materials and Solar Cells 176 (2018) 81–92.

[30] A. Anders, Energetic deposition using filtered cathodic arc plasmas, Vacuum. 67 (2002) 673–686

[31] J.M. Andersson, J. Vetter, J. Müller, J. Sjölén, Structural effects of energy input during growth of $Ti1-xAlxN$ (0.55≤x≤0.66) coatings by cathodic arc evaporation, Surf. Coatings Technol. 240 (2014) 211–220.

[32] A. Hörling, L. Hultman, M. Odén, J. Sjölén, L. Karlsson, Thermal stability of arc evaporated high aluminum-content $Ti1-xAlxN$ thin films, J. Vac. Sci. Technol. A Vacuum, Surfaces, Film. 20 (2002) 1815.

[33] N.P. Barradas, C. Jeynes, R.P. Webb, Simulated annealing analysis of Rutherford backscattering data, Appl. Phys. Lett. 71 (1997) 291.

[34] W. Theiss, CODE Manual. Optical Spectrum Simulation, (2007). http://www.wtheiss.com/.

Supplementary Information

S.1.- Variations in solar absorptance ($\Delta\alpha$) and thermal emittance ($\Delta\varepsilon$) of the SSC multilayers based on $Al_yTi_{1-y}(O_xN_{1-x})$ after the single-stage thermal tests. The performance criteria (PC) per multilayer and thermal treatment are also shown.

	Multilayer 1			Multilayer 2		
Temperature (ºC)	$\Delta\alpha$ (%)	$\Delta\varepsilon$(%)	PC(%)	$\Delta\alpha$(%)	$\Delta\varepsilon$(%)	PC(%)
450	-0.3	0.3	0.5	-0.8	-1.6	0.0
650	-2.2	2.7	3.6	0.3	-3.1	-1.9
800	-15.6	25.6	28.4	-12.6	25.2	25.2

S.2.- Variations in solar absorptance (α) and thermal emittance (ε) of the SSC multilayers after the cycling thermal tests. The performance criteria (PC) per multilayer and thermal treatment are also shown.

	Multilayer1			Multilayer 2		
# Cycles	$\Delta\alpha$ (%)	$\Delta\varepsilon$(%)	PC(%)	$\Delta\alpha$(%)	$\Delta\varepsilon$(%)	PC(%)
50	-0.2	0.1	0.3	1.7	-8.3	-5.9
100	-0.1	0.6	0.4	1.6	-0.4	-1.8
150	-0.3	1.0	0.8	1.0	3.3	0.7
200	-0.7	3.0	2.2	-0.2	5.7	3.1
250	-1.0	3.9	3.0	-0.4	5.4	3.1
300	-2.5	6.0	5.0	-3.7	11.6	9.5

S.3.- (a) SEM top view of multilayer 1 after symmetrical thermal cycling tests. (b) Zoom-in of oxide particles observed in (a). EDX elemental mapping of selected area in (a) presenting (c) Al, (d) Ti, (e) O and (f) Ni.